Neurobiology. In the article "On the spurious endoproteolytic processing of the presenilin proteins in cultured cells and tissues" by Nazneen N. Dewji, Chau Do, and S. J. Singer, which appeared in number 25, December 9, 1997, of *Proc. Natl. Acad. Sci. USA* (**94,** 14031–14036), the following correction should be noted. Lane 11 of Fig. 1*A* has been replaced. The revised Fig. 1*A* is printed below. This correction does not change the paper in any other way; in particular, the legend to Fig. 1 remains the same.

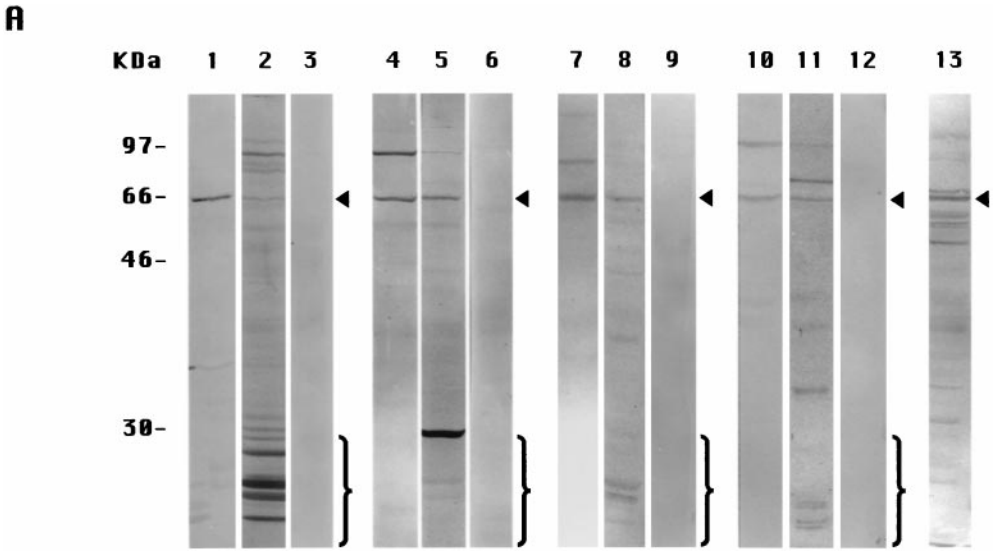

Neurobiology. In the article "*N*-Methyl-D-aspartate receptor activation and visual activity induce elongation factor-2 phosphorylation in amphibian tecta: A role for *N*-methyl-D-aspartate receptors in controlling protein synthesis" by A. J. Scheetz, Angus C. Nairn, and Martha Constantine-Paton, which appeared in number 26, December 23, 1997, of *Proc. Natl. Acad. Sci. USA* (**94,** 14770–14775), the authors have requested that their figures be reproduced because of poor quality on first publication. For clarity and continuity, all figures and legends are reprinted.*

*The layout of figures in this correction differs from the original layout.

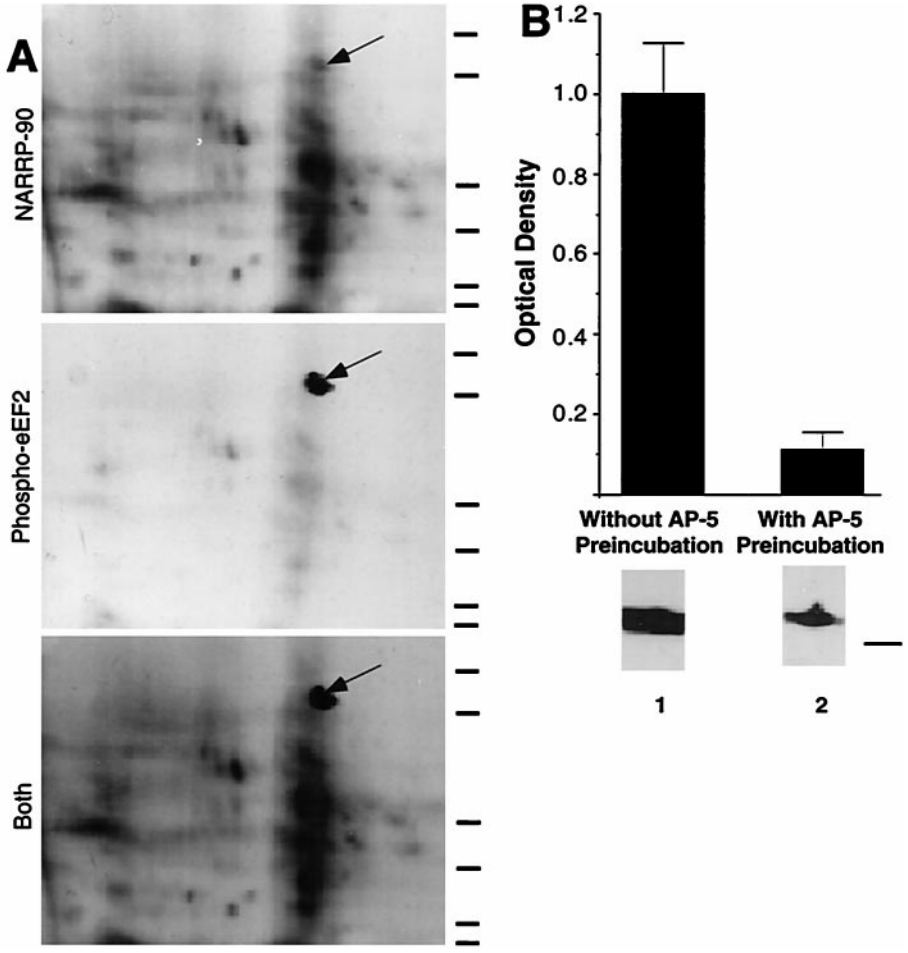

FIG. 1. NARPP-90 and eEF2 comigrate on blots of two-dimensional gels. (*A*) NARPP-90 phosphorylation was induced in tadpole tecta by NMDA/GLUT stimulation, the labeled proteins were blotted onto nitrocellulose, and NARPP-90 was detected by autoradiography (*Top*). The same blot was then probed with a phospho-specific anti-eEF2 antibody and the signal was detected with chemiluminescence (*Middle*). When a film was allowed to expose overnight after chemiluminescent detection, an image was produced that contained both radioactive and chemiluminescent signals (*Bottom*). This image shows that NARPP-90 and eEF2 have identical molecular masses and isoelectric points. Similar results were obtained in three other experiments. Molecular mass standards from bottom to top for each panel are 7.5, 18.2, 31.5, 42.7, 80, and 135 kDa. (*B*) Densitometric measurement of immunoblots detecting NMDAR-induced phospho-eEF2. Tecta received NMDA/GLUT stimulation with or without prior preincubation with 60 μM AP5. NMDA/GLUT stimulation alone resulted in a 7-fold increase in phospho-eEF2 compared with AP5 control ($n = 5$). NMDA/GLUT stimulation without AP5 preincubation produced robust eEF2 phosphorylation (lane 1). However, NMDA/GLUT stimulation after AP5 preincubation resulted in low levels of eEF2 phosphorylation (lane 2). To verify equal amounts of total eEF2 protein, all blots probed with the phospho-specific antibody were subsequently stripped and reprobed with the eEF2 antibody that does not distinguish between phospho- and dephospho-eEF2. The total amount of eEF2 did not vary as a function of stimulation (data not shown). The molecular mass standard for *B* is 80 kDa.

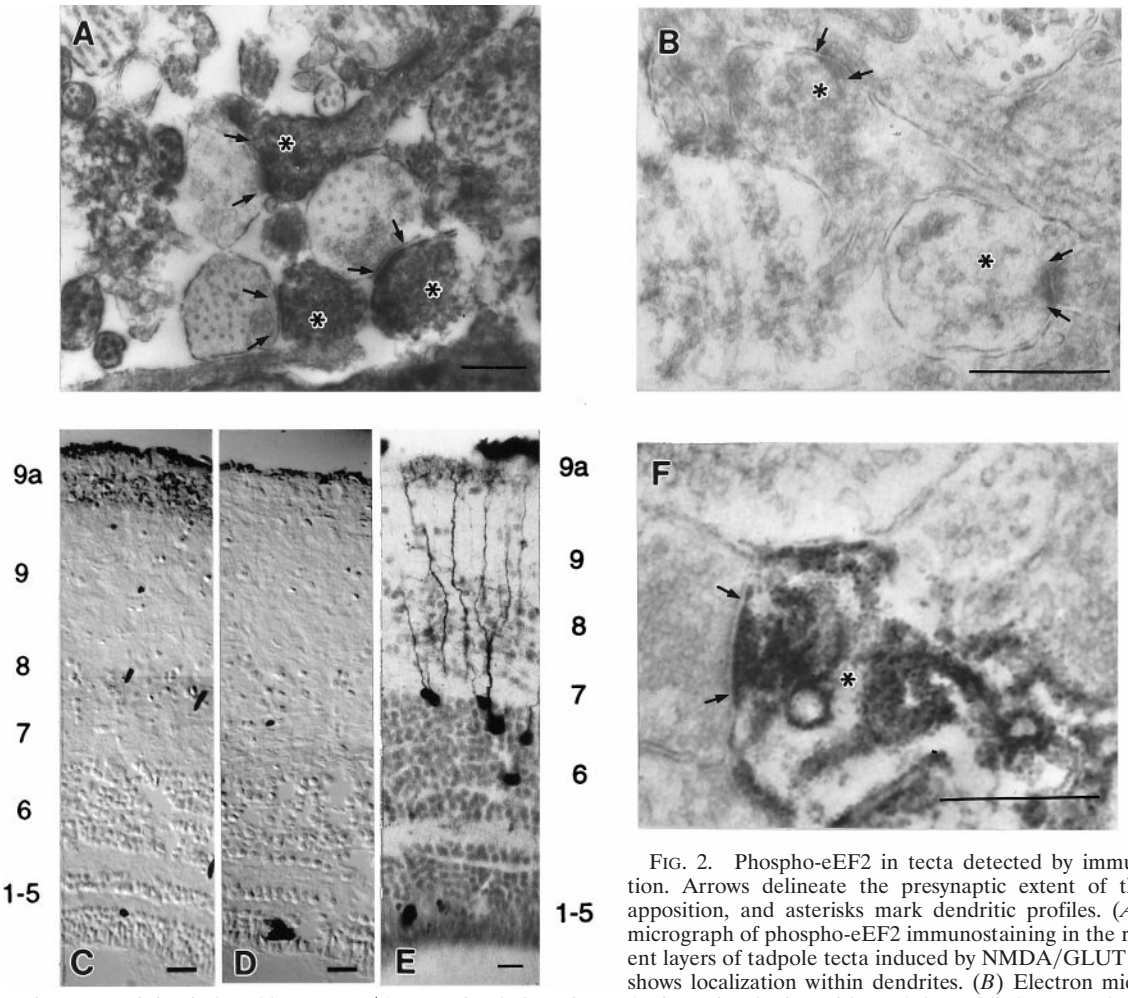

FIG. 2. Phospho-eEF2 in tecta detected by immunolocalization. Arrows delineate the presynaptic extent of the synaptic apposition, and asterisks mark dendritic profiles. (*A*) Electron micrograph of phospho-eEF2 immunostaining in the retinorecipient layers of tadpole tecta induced by NMDA/GLUT stimulation shows localization within dendrites. (*B*) Electron micrograph of phospho-eEF2 immunostaining induced by NMDA/GLUT stimulation after a 5-min preincubation with AP5 showed little or no phospho-eEF2. (*C*) Light-level micrograph of phospho-eEF2 immunostaining induced in adult frog tecta by NMDA/GLUT stimulation. (*D*) Light-level micrograph of phospho-eEF2 immunostaining in adult frog that received AP5 preincubation before NMDA/GLUT stimulation. No neuronal phospho-eEF2 staining was observed. (*E*) Tectal neurons that receive indirect ipsilateral retinal input via the nucleus isthmus have dense dendritic trees within layer 9a. Note that the layer labels for *C* and *D* correspond to the numbering on the left and the layers for *E* are on the right. (*F*) Electron micrograph of phospho-eEF2 immunostaining in adult frog tecta induced by NMDA/GLUT stimulation. This stimulation in adult tecta leads to preferential localization of phospho-eEF2 within dendritic segments subjacent to synaptic contacts in layer 9a. Pictures shown are representative of at least five independent determinations. Scale bars for *A*, *B*, and *F* represent 0.5 μm. Scale bars for *C–E* represent 50 μm.

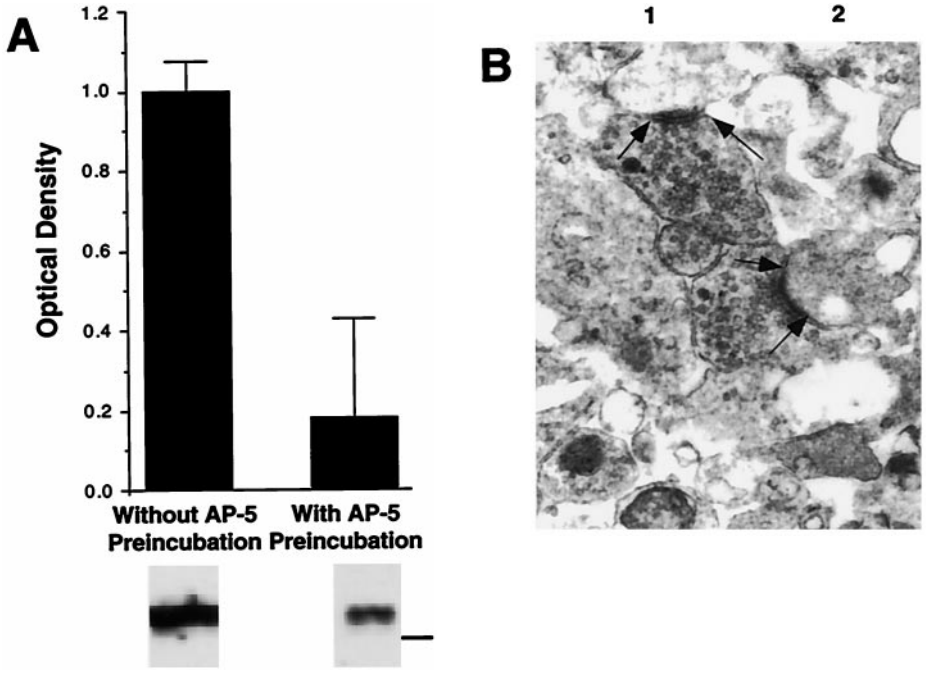

FIG. 3. Phospho-eEF2 is induced by NMDA/GLUT stimulation in preparations enriched in functional synaptic contacts. (*A*) Densitometric measurement of immunoblots detecting NMDAR-induced phospho-eEF2. Synaptoneurosomes received NMDA/GLUT stimulation with or without prior preincubation with 60 μM AP5. NMDA/GLUT stimulation alone resulted in a 7-fold increase in phospho-eEF2 compared with AP5 control. Examples shown are representative of three independent determinations. NMDA/GLUT stimulation without AP5 preincubation produced robust eEF2 phosphorylation (lane 1). However, NMDA/GLUT stimulation after AP5 preincubation resulted in low levels of eEF2 phosphorylation (lane 2). (*B*) Electron micrographs show that synaptoneurosomes are enriched in synaptic contacts. Arrows delineate presynaptic extent of synaptic apposition. Similar results were obtained from three independent synaptoneurosome preparations, and synaptic density is comparable to that reported previously (19).

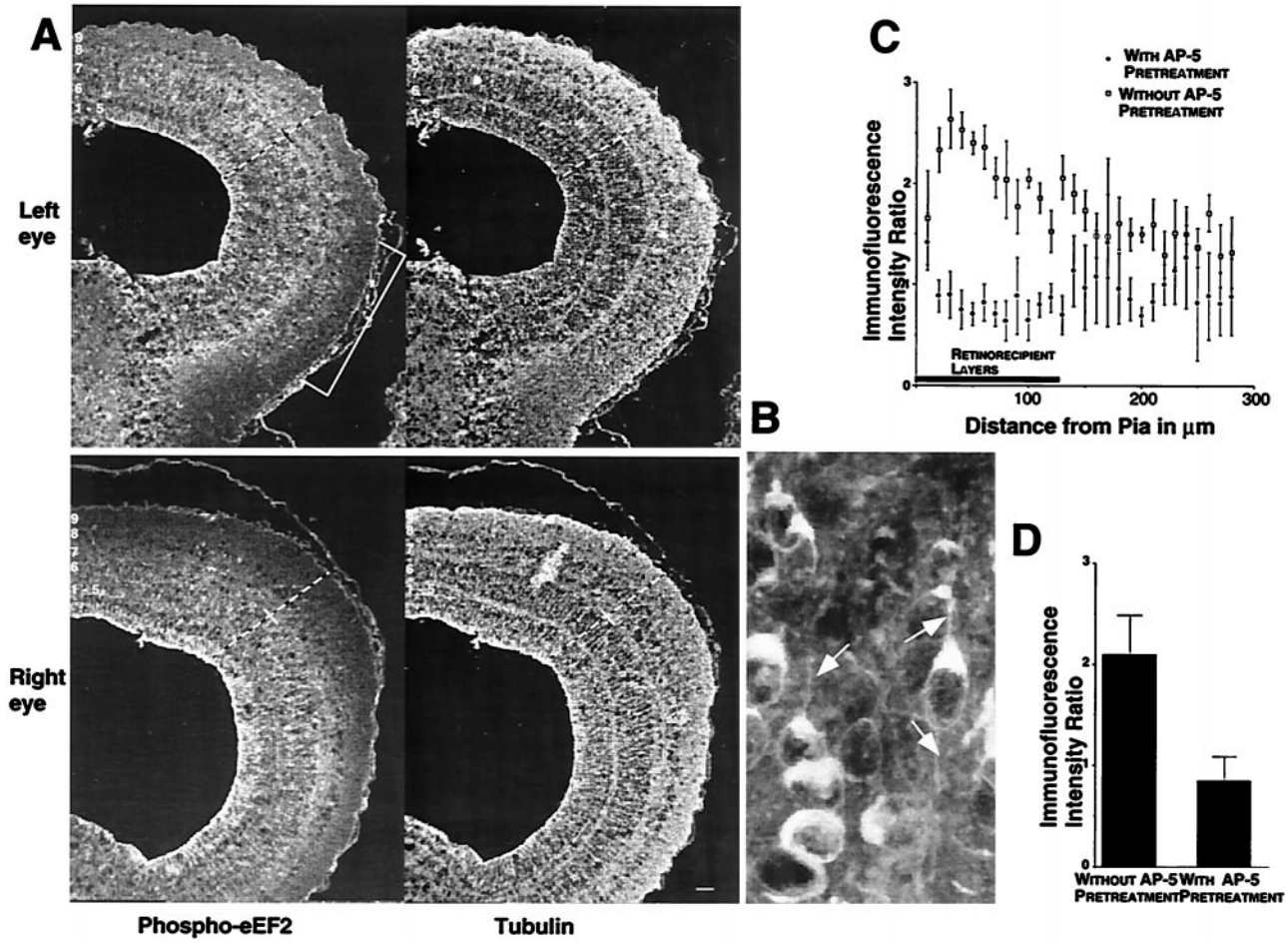

FIG. 4. Patterned visual stimulation causes eEF-2 phosphorylation within retinorecipient layers of the tadpole tectum. (*A*) Sections from tecta receiving either activated (*Upper*, left eye) or silenced (*Lower*, right eye) retinal input were stained for both phospho-eEF2 (*Left*, FITC) and tubulin (*Right*, Texas red). The white numbers indicate the location of the tectal layers. The dashed lines show representative line scans used for sampling fluorescence intensity. The small cross-hairs mark the boundary between the retinorecipient layers, 7–9, and the rest of the tectal layers. The white bracket shows the location of the ventral visual field projection that was shaded from the strobe and moving bar stimuli. This area of tectum provides an estimate of phospho-eEF2 levels caused by active but not directly stimulated retinal input. Signals for each fluorophore were imaged simultaneously from a single section. (*B*) A high magnification of tectal neurons and dendritic segments that are positive for eEF2 phosphorylation resulting from visual stimulation. Note the scattered punctate staining, which represents fine dendritic processes (arrows). (*C*) Laminar distribution of the ratio of phospho-eEF2 fluorescent signal in stimulated and silenced inputs in the absence (open squares) and presence (solid diamonds) of topically applied 60 μM AP5. The average location of retinorecipient layers is indicated by the bar along the abscissa. Error bars show the standard deviation of the average value from 5-pixel bins. (*D*) Histogram plots of the average ratio of phospho-eEF2 fluorescent signal between stimulated and silenced retinorecipient layers in the absence and presence of topically applied AP5. Error bars are the standard deviation derived from the average values for each individual used in the analysis ($n = 3$ with AP5 and $n = 5$ without AP5). Scale bar for *A* represents 50 μm.